ISSN 1674-1056
http://cpb.iphy.ac.cn
http://iopscience.iop.org/cpb
中国物理 B
Chinese Physics
中国物理 Chinese Physics B

Giant low-field magnetocaloric effectc in $EuTi_{1-x}Nb_xO_3$ (x=0.05, 0.1, 0.15, and 0.2) compounds

Wen-Hao Jiang(姜文昊), Zhao-Jun Mo(莫兆军), Jia-Wei Luo(罗佳薇), Zhe-Xuan Zheng(郑哲轩), Qiu-Jie Lu(卢秋杰), Guo-Dong Liu(刘国栋), Jun Shen(沈俊), Lan Li(李岚)

Citation: Chin. Phys. B . 2020, 29(3): 037502 . **doi:** 10.1088/1674-1056/ab69e7
Journal homepage: http://cpb.iphy.ac.cn; http://iopscience.iop.org/cpb

What follows is a list of articles you may be interested in

Magnetoresistance hysteresis in topological Kondo insulator SmB_6 nanowire

Ling-Jian Kong(孔令剑), Yong Zhou(周勇), Hua-Ding Song(宋化鼎), Da-Peng Yu(俞大鹏), Zhi-Min Liao(廖志敏)
Chin. Phys. B . 2019, 28(10): 107501 . **doi:** 10.1088/1674-1056/ab3a89

Critical behavior and magnetocaloric effect in magnetic Weyl semimetal candidate $Co_{2-x}ZrSn$

Tianlin Yu(于天麟), Xiaoyun Yu(余骁昀), En Yang(杨恩), Chang Sun(孙畅), Xiao Zhang(张晓), Ming Lei(雷鸣)
Chin. Phys. B . 2019, 28(6): 067501 . **doi:** 10.1088/1674-1056/28/6/067501

Magnetic properties and magnetocaloric effects in $(Ho_{1-x}Y_x)_5Pd_2$ compounds

X F Wu(武小飞), C P Guo(郭翠萍), G Cheng(成钢), C R Li(李长荣), J Wang(王江), Y S Du(杜玉松), G H Rao(饶光辉), Z M Du(杜振民)
Chin. Phys. B . 2019, 28(5): 057502 . **doi:** 10.1088/1674-1056/28/5/057502

Ferromagnetism and magnetostructural coupling in V-doped MnNiGe alloys

Hui Yang(杨慧), Jun Liu(刘俊), Chao Li(李超), Guang-Long Wang(王广龙), Yuan-Yuan Gong(龚元元), Feng Xu(徐锋)
Chin. Phys. B . 2018, 27(10): 107502 . **doi:** 10.1088/1674-1056/27/10/107502

Magnetostructural transformation and magnetocaloric effect in $Mn_{48-x}V_xNi_{42}Sn_{10}$ ferromagnetic shape memory alloys

Najam ul Hassan, Ishfaq Ahmad Shah, Tahira Khan, Jun Liu(刘俊), Yuanyuan Gong(龚元元), Xuefei Miao(缪雪飞), Feng Xu(徐锋)
Chin. Phys. B . 2018, 27(3): 037504 . **doi:** 10.1088/1674-1056/27/3/037504

Giant low-field magnetocaloric effect in $EuTi_{1-x}Nb_xO_3$ ($x = 0.05$, 0.1, 0.15, and 0.2) compounds*

Wen-Hao Jiang(姜文昊)[1], Zhao-Jun Mo(莫兆军)[1,†], Jia-Wei Luo(罗佳薇)[1], Zhe-Xuan Zheng(郑哲轩)[1], Qiu-Jie Lu(卢秋杰)[1], Guo-Dong Liu(刘国栋)[3], Jun Shen(沈俊)[2], and Lan Li(李岚)[1,‡]

[1] *School of Material Science and Engineering, Institute of Material Physics, Key Laboratory of Display Materials and Photoelectric Devices of Ministry of Education, Key Laboratory for Optoelectronic Materials and Devices of Tianjin, Tianjin University of Technology, Tianjin* 300191, *China*

[2] *Key Laboratory of Cryogenics, Technical Institute of Physics and Chemistry, Chinese Academy of Sciences, Beijing* 100190, *China*

[3] *School of Material Science and Engineering, Hebei University of Technology, Tianjin* 300401, *China*

(Received 14 October 2019; revised manuscript received 2 January 2020; accepted manuscript online 10 January 2020)

The magnetic properties and magnetocaloric effect (MCE) of $EuTi_{1-x}Nb_xO_3$ ($x = 0.05$, 0.1, 0.15, and 0.2) compounds are investigated. Owing to electronic doping, parts of Ti ions are replaced by Nb ions, the lattice constant increases and a small number of Ti^{4+} ($3d^0$) ions change into Ti^{3+} ($3d^1$). It is the ferromagnetism state that is dominant in the derivative balance. The values of the maximum magnetic entropy change ($-\Delta S_M^{max}$) are 10.3 J/kg·K, 9.6 J/kg·K, 13.1 J/kg·K, and 11.9 J/kg·K for $EuTi_{1-x}Nb_xO_3$ ($x = 0.05$, 0.1, 0.15, and 0.2) compounds and the values of refrigeration capacity are 36, 33, 86, and 80 J/kg as magnetic field changes in a range of 0 T–1 T. The $EuTi_{1-x}Nb_xO_3$ ($x = 0.05$, 0.1, 0.15, and 0.2) compounds with giant reversible MCE are considered as a good candidate for magnetic refrigerant working at low-temperature and low-field.

Keywords: magnetocaloric effect, magnetic entropy change, magnetic phase transformation

PACS: 75.30.Sg, 65.40.gd, 75.30.Kz **DOI:** 10.1088/1674-1056/ab69e7

1. Introduction

Liquid helium temperature zones are widely used in low temperature physics, superconducting technology, aerospace, and so on.[1] Magnetic refrigeration technology is one of the high efficiency refrigeration techniques and can be applied to extreme research environment.[2] Magnetocaloric effect materials are the core of magnetic refrigeration technology. Currently, the rare earth intermetallic compounds are a larger family in a low temperature region, such as $DyCo_2Si_2$,[3] $ReFe_2Si_2$ (Re = Pr and Nd),[4] ErCoSn,[5] Er_4CoCd,[6] Tm_4CoCd,[7] Re_2CuSi_3 (Re = Dy and Ho),[8] HoCoAl,[9] the quaternary compound ReT_2B_2C (where Re represents a rare earth element and T a transition metal),[10] *etc*.

Recently, rare earth metal oxides are gradually becoming another important research direction of the low-temperature magnetocaloric materials, such as $ReCrO_4$ (Re = Ho, Gd, Lu),[11] Pr_2CoMnO_6,[12] Re_2BaCuO_5 (Re = Dy and Er).[13] Li *et al.* reported that when the magnetic field changed from 0 T to 5 T, the maximum values of magnetic entropy change (ΔS_M^{max}) could reach 7.5 J/kg·K and 9.2 J/kg·K for $Dy_2Cu_2O_5$ and $Ho_2Cu_2O_5$ respectively.[14] Balli *et al.* reported the anisotropic magnetocaloric effect in single-crystal $HoMn_2O_5$, the value of $-\Delta S_M^{max}$ was 13.1 J/kg·K in the easy axis direction as the change of magnetic field (ΔH) is 0 T–7 T.[15] In 2016, Koushik Dey *et al.* reported that $ReVO_4$ compounds also exhibited huge value of ΔS_M at low temperature. The values of $-\Delta S_M^{max}$ were 41.1 J/kg·K, 7.94 J/kg·K, and 19.7 J/kg·K for $GdVO_4$, $HoVO_4$, and $ErVO_4$ when ΔH = 5 T.[16]

Around the temperature region of liquid helium, the magnetic order arrangement of the Cubic perovskite material $EuTiO_3$ is G-type antiferromagnetic (AFM).[17] In $EuTiO_3$, Ti is tetravalent ($3d^0$) and Eu is divalent with large spin moment ($S = 7/2$) caused by the stable $4f^7$ electronic configuration. The single crystal $EuTiO_3$ shows a large reversible magnetocaloric effect, the value of ΔS_M^{max} is 42.4 J/kg·K as $\Delta H = 5$ T.[18] The polycrystalline $EuTiO_3$ also shows a large $-\Delta S_M^{max}$.[19] Previous reports indicate that the improvement of ferromagnetism (FM) exchange could effectively increase the $-\Delta S_M$ around the transition temperature when $\Delta H = 1$ T, such as $Eu_{1-x}Ba_xTiO_3$ (11.6 J/kg·K),[20] $Eu_{1-x}Sr_xTiO_3$ (10 J/kg·K),[21] $Eu_{1-x}La_xTiO_3$ (10.8 J/kg·K),[22] and $EuTi_{0.9}V_{0.1}O_3$ (11 J/kg·K).[23] When parts of Ti ions are substituted by Nb ions, the magnetic state changes into FM metallic state.[24,25] In 2016, Roy *et al.* reported that a large magnetocaloric effect of single crystal $EuTi_{0.85}Nb_{0.15}O_3$ (14.7 J/kg·K) could be obtained when $\Delta H = 1$ T. Roy speculated the Nb^{4+} ($4d^1$) in the $EuTi_{0.85}Nb_{0.15}O_3$ based on metallic behavior.[26] The introduction of an itinerant electron me-

*Project supported by the Science & Technology Development Fund of Tianjin Education Commission for Higher Education, China (Grant No. 2017KJ247).

†Corresponding author. E-mail: mzjmzj163@163.com

‡Corresponding author. E-mail: lilan@tjut.edu.cn

© 2020 Chinese Physical Society and IOP Publishing Ltd

diates the Ruderman–Kittel–Kasuya–Yosida (RKKY) interaction between the localized moments of Eu^{2+} ions and the system and exhibits ferromagnetic effect above a critical value of Nb concentration.[24,25] But, if the Nb ions exhibit Nb^{5+} ($4d^0$), it is also possible to introduce an itinerant electron occupying an empty orbit of the Ti 3d state, resulting in a decrease in Eu 4f–Ti 3d–Eu 4f hybridization and the suppression of AFM coupling, because the AFM exchange comes from the superexchange of Eu^{2+} 4f spins via the Ti^{4+} 3d states.[27] For $EuTi_{1-x}Nb_xO_3$ compounds, the contribution of increasing FM exchange needs to be further confirmed and the magnetocaloric effect needs to be studied systematicly.

In this study $EuTi_{1-x}Nb_xO_3$ ($x = 0.05$, 0.1, 0.15, and 0.2) compounds are obtained by introducing Nb^{5+} ions into $EuTiO_3$. The value of $-\Delta S_M^{max}$ is 13.1 J/kg·K for $EuTi_{0.85}Nb_{0.15}O_3$ when $\Delta H = 1$ T, which is more greatly improved than that for $EuTiO_3$. The improvement of ΔS_M is attributed to the increase of FM exchange due to the electron doping and lattice expansion in the $EuTiO_3$.

2. Experimental section

A series of $EuTi_{1-x}Nb_xO_3$ ($x = 0.05$, 0.1, 0.15, and 0.2) compounds are prepared by sol–gel method in this work. Firstly, europium oxide (Eu_2O_3) and five niobium chlorides ($NbCl_5$) are added to an aqueous solution of nitric acid according to a stoichiometric ratio and stirred until they are completely dissolved. Next, tetrabutyl titanate ($Ti(OC_4H_9)_4$) is added and stirred for 0.5 h to clarify. Secondly, ethylene glycol ($C_2H_6O_2$) is added as dispersant and stirred for 0.5 h. Then the configured homogeneous solution is dried at 353 K and thoroughly ground. Finally, the power sample is sintered in a tube furnace at 1373 K for 3 h to obtain the precursor, next the precursor is sintered in mixed gas (8% H_2 and 92% Ar) at 1573 K for 5 h to obtain $EuTi_{1-x}Nb_xO_3$ ($x = 0.05$, 0.1, 0.15, and 0.2) series of samples.

The structures of $EuTi_{1-x}Nb_xO_3$ compounds are determined by a Rigaku 2500/PC x-ray diffractometer with a Cu $K\alpha$ radiation source, and the wavelength was 1.54184 Å. The element valence is confirmed by x-ray photoelectron spectroscopy (XPS, ESCALAB 250Xi). The isothermal magnetization curves are measured by using a commercial superconducting quantum interference device (SQUID) magnetometer and model MPMS-7 from Quantum Design Inc.

3. Results and discussion

Figure 1 shows XRD diffraction peak for each of $EuTi_{1-x}Nb_xO_3$ ($x = 0.05$, 0.1, 0.15, and 0.2) compounds, indicating that the $EuTi_{1-x}Nb_xO_3$ ($x = 0.05$, 0.1, 0.15, and 0.2) are single-phase crystals and belong to a cubic perovskite structure (space group 221). The refined lattice parameter increases from 3.9055 Å to 3.9273 Å with doping Nb ions increasing as shown in the inset of Fig. 1. It is attributed to the larger size of Nb ions (~ 0.69 Å), after Ti ions have been replaced by Nb ions.

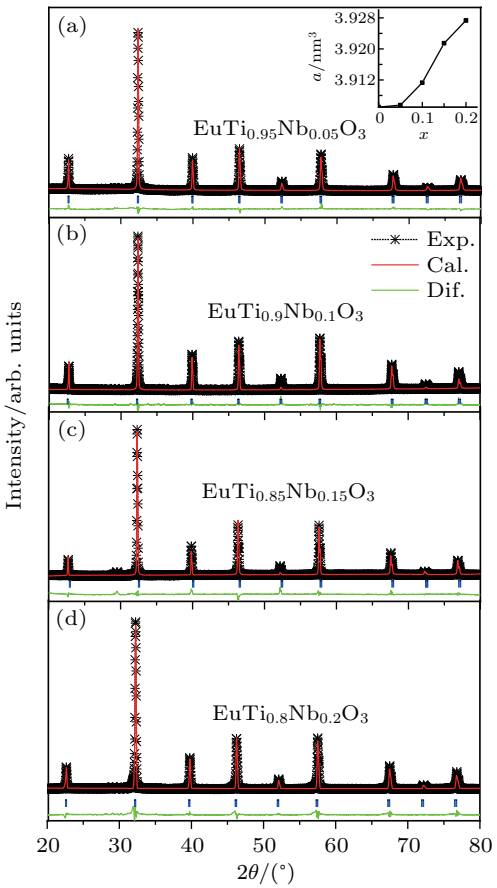


Fig. 1. XRD patterns of $EuTi_{1-x}Nb_xO_3$ ($x = 0.05$, 0.1, 0.15, and 0.2) compounds. Observed data are denoted by crosses, and calculated profile is continuous line overlying them. Short vertical lines indicate angular positions of Bragg positions, and the green curve is the difference between the experimental data and the calculated data. Illustration shows variation of cell volume.

In order to determine the valence of Nb ion in the $EuTi_{1-x}Nb_xO_3$ ($x = 0.05$, 0.1, 0.15, and 0.2) compounds, figures 2(a) and 2(b) show the XPS spectra of Nb 3d and Ti 2p for $EuTi_{1-x}Nb_xO_3$ ($x = 0.05$, 0.1, 0.15, and 0.2) compounds. There are dual positions for Nb 3d (Nb $3d^{3/2}$ and Nb $3d^{5/2}$), and Nb $3d^{5/2}$ is 206.5–206.9 corresponding to the chemical valence of Nb^{5+}, which is different from the previously reported value of Nb^{4+}.[24] The Ti^{3+} was observed in the XPS due to the balance of the valence state.

Figure 3 shows the zero-field-cooling (ZFC) and the field-cooling (FC) temperature dependence of magnetization for $EuTi_{1-x}Nb_xO_3$ ($x = 0.05, 0.1, 0.15$, and 0.2) compounds under an applied magnetic field of 0.01 T. With the decrease of temperature, $EuTi_{1-x}Nb_xO_3$ compounds experience a change from paramagnetic (PM) state to FM state, which are different from what $EuTiO_3$ compound does. The transition temperature of $EuTi_{1-x}Nb_xO_3$ compound is determined according to the dM/dT as shown in the inset of Fig. 3. When the tem-

perature is higher than the phase transition temperature, the thermal hysteresis is observed in none of the samples. And a bifurcation is observed below transition temperature, which is probably caused by a domain wall pinning effect. But the bifurcation decreases with the number of Nb ions substituting for Ti ions, which may be attributed to the enhancement of FM coupling. Previous reports explained that Nb doping induced ferromagnetism, which is most likely to result from the ferromagnetic interaction between localized Eu-4f spins, mediated by itinerant electrons introduced by chemical doping.[28] The FM ordering of the localized Eu^{2+} spin is mediated by the itinerant electrons of the dopant Nb^{4+} ($4d^1$).[26] However, the Nb ions exhibit Nb^{5+} as shown in XPS, which maybe introduces t_{2g}^1 electrons into the empty Ti-3d band such as $Eu_{1-x}La_xTiO_3$ compounds.[22] In $EuTiO_3$ the antiferromagnetic coupling comes from the superexchange interactions with Ti-3d (t_{2g}) empty states.[27] Therefore, the $3d^1$ of Ti ions maybe suppresses antiferromagnetic coupling and promotes ferromagnetic interaction between 4f spins neighboring Eu^{2+} ions through RKKY. What is more, Akamatsu *et al*. reported that the increase of lattice parameters in $Eu_{1-x}Ba_xTiO_3$[20] and $Eu_{1-x}Sr_xTiO_3$[21] could improve the FM coupling.[27] The ionic radius of Nb^{5+} is larger than that of Ti^{4+} which obviously increases the lattice constant as shown by XRD in Fig. 1. In short, there are two factors that could improve FM exchange: electronic doping and lattice expansion.

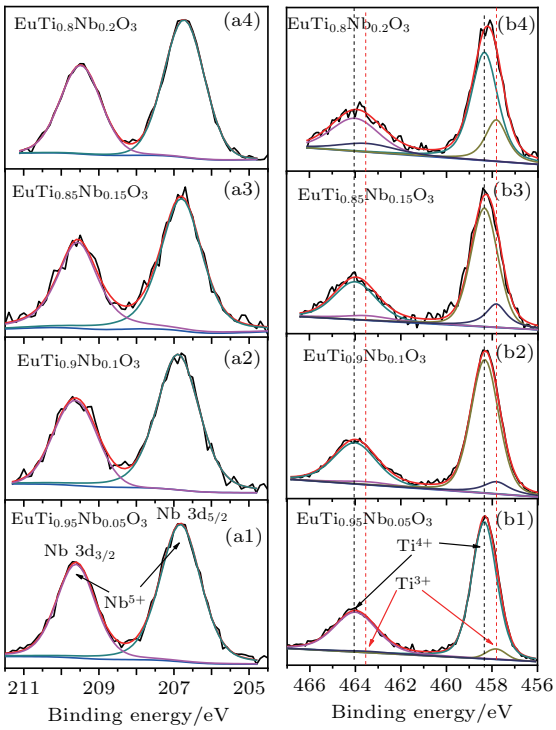


Fig. 2. XPS spectra of Nb 3d and Ti 2p for $EuTi_{1-x}Nb_xO_3$ ($x = 0.05$, 0.1, 0.15, and 0.2) compounds.

Figure 4 shows the isothermal magnetization curves in a temperature range from 3 K to 28 K under magnetic fields ranging from 0 kOe to 50 kOe (1 Oe = 79.5775 $A{\cdot}m^{-1}$). The isothermal magnetization curves of $EuTi_{1-x}Nb_xO_3$ compounds are nonlinear when $T_C < T < 16$ K, indicating the existence of short-range FM state in the paramagnetic state. None of the isothermal magnetization curves crosses with other one in a low magnetic field range of 0 kOe–10 kOe at 3 K, 4 K, 5 K, and 6 K as shown in Fig. 5, which also implies that the $EuTi_{1-x}Nb_xO_3$ compounds all present the FM state.

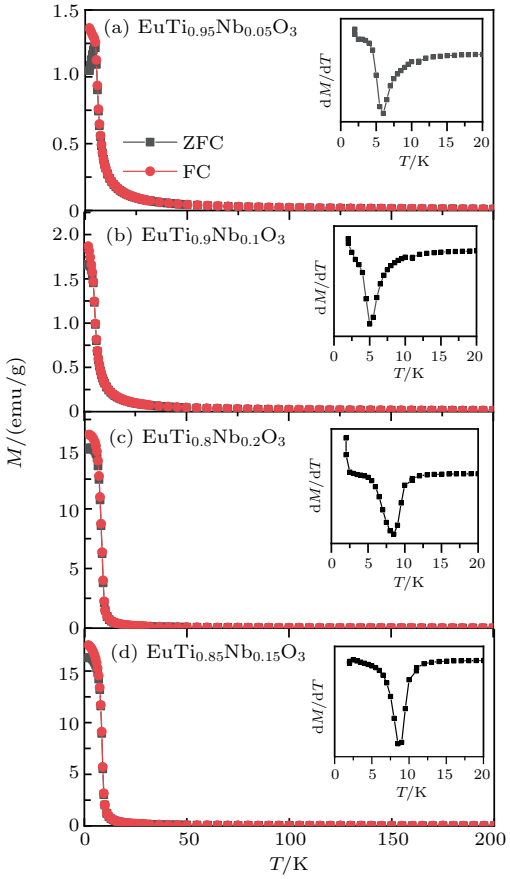


Fig. 3. Temperature-dependent magnetization M curves of ZFC and FC for $EuTi_{1-x}Nb_xO_3$ ($x = 0.05$, 0.1, 0.15, and 0.2) under magnetic field of 0.01 T, with inserts showing dM/dT *versus* T curves at low temperature under magnetic field of 0.01 T.

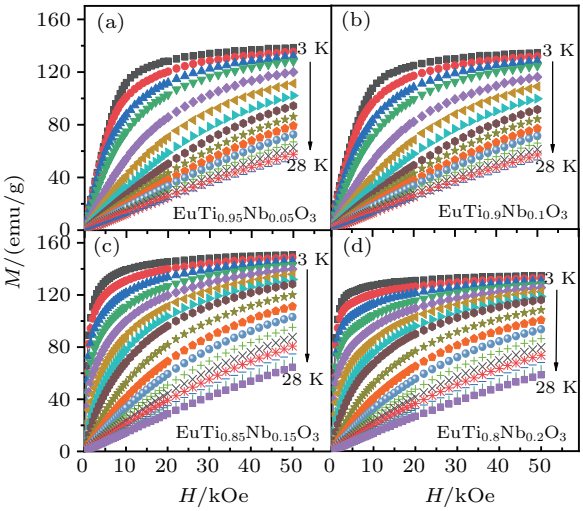


Fig. 4. Magnetization isotherms of $EuTi_{1-x}Nb_xO_3$ ($x = 0.05$, 0.1, 0.15, and 0.2) compounds measured in temperature range of 3 K–28 K under applied magnetic fields ranging from 0 kOe to 50 kOe.

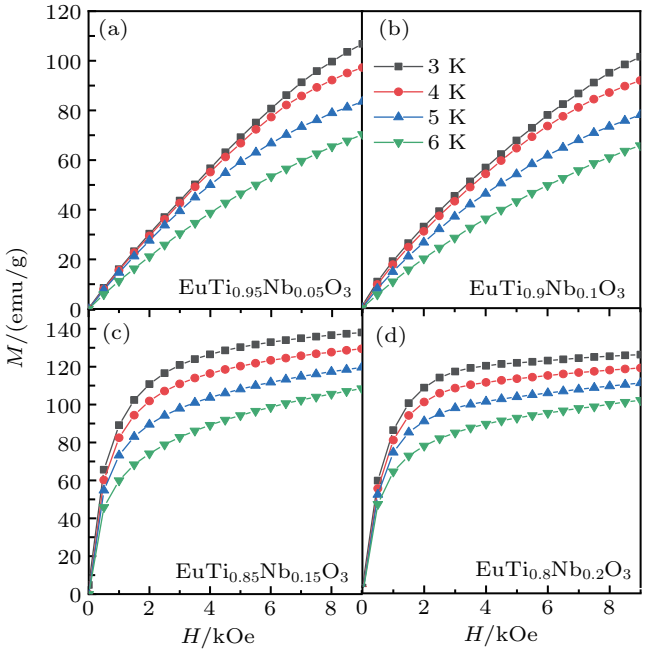


Fig. 5. Magnetization isotherms of $EuTi_{1-x}Nb_xO_3$ ($x = 0.05$, 0.1, 0.15, and 0.2) compounds measured in temperature range of 3 K, 4 K, 5 K, 6 K under applied magnetic fields ranging from 0 kOe to 10 kOe.

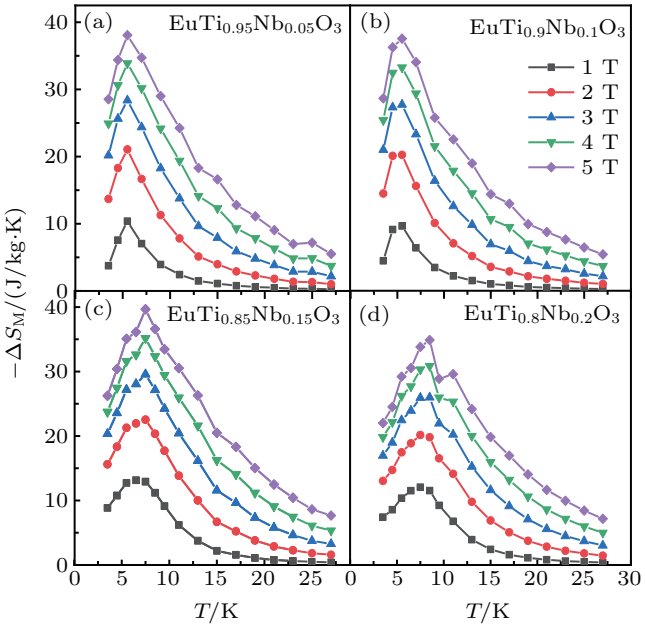


Fig. 6. Temperature-dependent magnetic entropy change under magnetic fields 1 T–5 T for $EuTi_{1-x}Nb_xO_3$ ($x = 0.05$, 0.1, 0.15, and 0.2) compounds.

According to the Maxwell relation $\Delta S(T,H) = \int_0^H (\partial M/\partial T)_H \mathrm{d}H$, the value of $-\Delta S_M$ is calculated by the isothermal magnetization curve.[29] Figure 6 shows the relationship between $-\Delta S_M$ and temperature for each of the $EuTi_{1-x}Nb_xO_3$ compounds when ΔH is in a range of 0 T–5 T. The values of $-\Delta S_M^{max}$ are 38.0 J/kg·K, 37.5 J/kg·K, 39.6 J/kg·K, and 34.6 J/kg·K, respectively, for $EuTi_{1-x}Nb_xO_3$ ($x = 0.05$, 0.1, 0.15, and 0.2) compounds at transition temperature when $\Delta H = 5$ T. Although the values of $-\Delta S_M$ for $EuTi_{1-x}Nb_xO_3$ compounds decrease when $\Delta H = 5$ T, the values of $-\Delta S_M$ are 13.1 J/kg·K and 11.9 J/kg·K, respectively, for $EuTi_{0.85}Nb_{0.15}O_3$ and $EuTi_{0.8}Nb_{0.2}O_3$ when $\Delta H = 1$ T, which are larger than that for $EuTiO_3$ (9.8 J/kg·K). The values of $-\Delta S_M$ for these compounds are all greater than those for other rare earth metal oxide compounds near the liquid helium temperature, such as R_2NiMnO_6 (R = Dy, Ho, and Er),[30] $GdMnO_3$,[31] and $DyScO_3$,[32] and so on. The increase of $-\Delta S_M$ may be attributed to the enhancement of FM exchange due to electronic doping and crystal lattice expansion.

In practical application, magnetic refrigeration materials need not only a large $-\Delta S_M$, but also a wide range of phase change temperature, so that they can ensure better cooling effect in a sufficiently wide operating temperature range. The refrigeration capacity (*RC*) is another important parameter. It represents the exchange of energy between heat and cold in the process of heat exchange, which is directly related to energy efficiency. The *RC* is calculated from $RC = \int_{T_2}^{T_1} |\Delta S_M| \, \mathrm{d}T$, where T_1 and T_2 are the temperatures corresponding to half of the peak for the integration limit. The values of *RC* and $-\Delta S_M$ for the $EuTi_{1-x}Nb_xO_3$ compounds and $EuTiO_3$ are shown in Table 1 when $\Delta H = 1$ T, 2 T, and 5 T. It could be observed that the *RC* values of the $EuTi_{1-x}Nb_xO_3$ compounds are larger than that of the $EuTiO_3$ compound. Especially under the magnetic field changing from 0 T to 1 T the values of *RC* are 86 J/kg and 80 J/kg for $EuTi_{0.85}Nb_{0.15}O_3$ and $EuTi_{0.8}Nb_{0.2}O_3$ respectively, which are three times larger than that for the $EuTiO_3$ (27 J/kg). It could be clearly observed that the $EuTi_{0.85}Nb_{0.15}O_3$ and $EuTi_{0.8}Nb_{0.2}O_3$ present FM and larger $-\Delta S_M$ under a low change of magnetic field. At the same time, the temperature span (the full width at half maximum of the $-\Delta S_M$) is expanded, so greatly improving the *RC*, which is more conducive to practical applications. In summary, the $EuTi_{1-x}Nb_xO_3$ compounds are considered as a good candidate for magnetic refrigeration materials in liquid helium temperature regions.

Table 1. Values of $-\Delta S_M$ and *RC* under field change of 1 T, 2 T, and 5 T for $EuTiO_3$, $EuTi_{1-x}Nb_xO_3$ ($x = 0.05$, 0.1, 0.15, and 0.2) compounds.

Samples	$-\Delta S_M$/(J/kg·K)		*RC*/(J/kg)		
	1 T	2 T	1 T	2 T	5 T
$EuTiO_3$	9.8	22.3	27	98	292
$EuTi_{0.95}Nb_{0.05}O_3$	10.3	21	36	104	307
$EuTi_{0.9}Nb_{0.1}O_3$	9.6	20.3	33	100	304
$EuTi_{0.85}Nb_{0.15}O_3$	13.1	22.6	86	174	397
$EuTi_{0.8}Nb_{0.2}O_3$	11.9	20	80	158	365

The second-order phase transition is more suitable for magnetic refrigeration cycles. Based on Banerjee's[33] criterion, if the Arrott plot has a positive slope, the magnetic transition is a second-order phase transition, while the negative slope or S-type belongs to the first-order phase transition.

The Arrott plots of the $EuTi_{1-x}Nb_xO_3$ compounds show positive slopes as shown in Fig. 7, indicating the second-order phase transition. The phenomenological universal curve of the $-\Delta S_M$ has been proposed as another method to distinguish between the second order phase transition and the first order phase transition.[34] The normalize $\Delta S'(\theta)$ can be folded into a curve under different magnetic fields. The reference temperature T_{r1} and T_{r2} correspond to the peak of $\Delta S_M/\Delta S_M^{max} = 0.5$. The temperature axis is rescaled in a different way below and above T_C as shown below:

$$\theta = \begin{cases} -(T-T_C)/(T_{r1}-T_C), & T \le T_C, \\ (T-T_C)/(T_{r2}-T_C), & T \ge T_C. \end{cases}$$

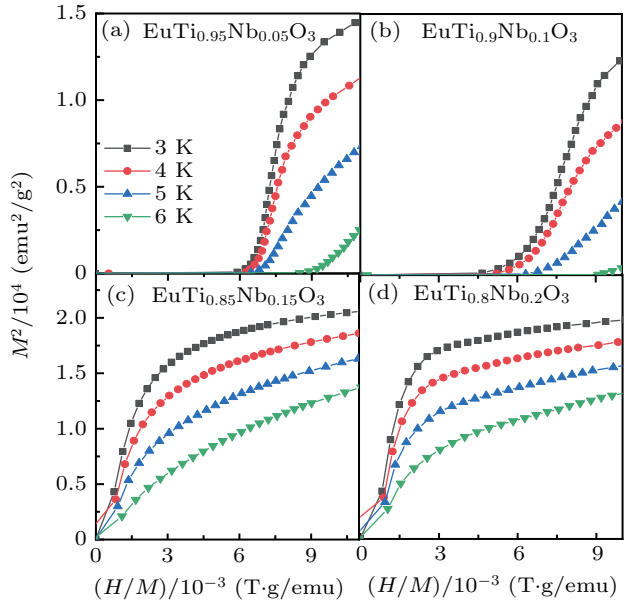


Fig. 7. Arrott plots of $EuTi_{1-x}Nb_xO_3$ ($x = 0.05$, 0.1, 0.15, and 0.2) compounds.

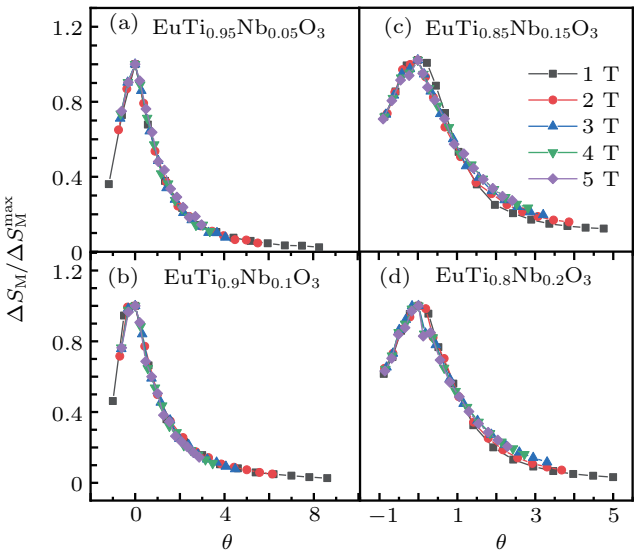


Fig. 8. θ-dependent $\Delta S'(T)$ for typical field changes in $EuTi_{1-x}Nb_xO_3$ ($x = 0.05$, 0.1, 0.15, and 0.2) compounds.

Figure 8 shows a $\Delta S'(\theta)$ plot of different magnetic fields for the $EuTi_{1-x}Nb_xO_3$ compounds. It can be observed that the $\Delta S'(\theta)$ curves almost overlap, which further prove the second-order phase transitions for $EuTi_{1-x}Nb_xO_3$ ($x = 0.05$, 0.1, 0.15, and 0.2) compounds.

4. Conclusions

A series of $EuTi_{1-x}Nb_xO_3$ ($x = 0.05$, 0.1, 0.15, and 0.2) compounds is prepared by the sol–gel method. The magnetic and magnetocaloric effects of compounds are studied. The compounds are of the cubic perovskite structure and the Nb element is confirmed to be pentavalent by XPS. The substitution of Nb^{5+} ions for Ti^{4+} ions increases the lattice constant and achieves electronic doping, which leads FM exchange to increase. The values of $-\Delta S_M^{max}$ for the $EuTi_{1-x}Nb_xO_3$ ($x = 0.05$, 0.1, 0.15, and 0.2) compounds are 10.3 J/kg·K, 9.6 J/kg·K, 13.1 J/kg·K, and 11.9 J/kg·K, values of *RC* are 36 J/kg, 33 J/kg, 86 J/kg, and 80 J/kg when $\Delta H = 1$ T, respectively. In addition, the $EuTi_{1-x}Nb_xO_3$ compounds all experience the second-order phase transitions without hysteresis loss. In summary, $EuTi_{1-x}Nb_xO_3$ compounds are considered as one of the most promising magnetic refrigeration materials in the liquid helium temperature zone.

References

[1] Benford S M and Brown G V 1981 *J. Appl. Phys.* **52** 2110
[2] Shen B G, Sun J R, Hu F X, Zhang H W and Cheng Z H 2009 *Adv. Mater.* **21** 4545
[3] Karmakar S K, Giri S and Majumdar S 2017 *J. Appl. Phys.* **121** 043901
[4] Ma Y H, Dong X S, Qi Y and Li L W 2018 *J. Magn. Magn. Mater.*
[5] Souza R L, Monteiro J C B, dos Santos A O, Cardoso L P and da Silva L M 2019 *J. Magn. Magn. Mater.* 165653
[6] Guo D, Wang Y M, Li H D, Guan R G, Xu H and Zhang Y K 2019 *J. Magn. Magn. Mater.* **489** 165462
[7] Li L W, Huo D X, Su K P and Pöttgen R 2018 *Intermetallics* **93** 343
[8] Zhang Y K, Guo D, Yang Y, Geng S H, Li X, Ren Z M and Wilde G 2017 *J. Alloys Compd.* **702** 546
[9] Zhang X X, Wang F W and Wen G H 2011 *J. Phys.: Condens. Matter* **13** L747
[10] Zheng X Q, Shen J, Hu F X, Sun J R and Shen B G 2016 *Acta Phys. Sin.* **65** 217502 (in Chinese)
[11] Midya A, Khan N, Bhoi D and Mandal P 2014 *J. Appl. Phys.* **115** 17E114
[12] Bhattia I N, Mahatob R N, Bhattib I N and Ahsan M A H 2019 *Physica B* **558** 59
[13] Li L W, Su K P and Huo D X 2018 *J. Alloys Compd.* **735** 773
[14] Li L W, Wang J, Su K P, Huo D X and Qi Y 2016 *J. Alloys Compd.* **658** 500
[15] Balli M, Jandl S, Fournier P and Gospodinov M M 2014 *Appl. Phys. Lett.* **104** 232402
[16] Dey K, Indra A, Majumdar S and Giri S 2017 *J. Mater. Chem.* **5** 1646
[17] Shvartsman V V, Borisov P, Kleemann W, Kamba S and Katsufuji T 2010 *Phys. Rev. B* **81** 064426
[18] Rubi K, Chen R F, Wang J S and Mahendiran R 2016 *Phys. Rev. B* **93** 094422
[19] Mo Z J, Shen J, Li L, Liu Y, Tang C C, Hu F X, Sun J R and B G Shen 2015 *Mater. Lett.* **158** 282
[20] Rubi K, Kumar P, Maheswar Repaka D V, Chen R F, Wang J S and Mahendiran R 2014 *Appl. Phys. Lett.* **104** 032407
[21] Mo Z J, Sun Q L, Wang C H, *et al.* 2016 *Ceram. Int.* **43** 2083

[22] Mo Z J, Sun Q L, Shen J, Yang M, *et al.* 2018 *Chin. Phys. B* **27** 017501
[23] Roy S, Das M and Mandal P 2018 *Phys. Rev. Mater.* **2** 064412
[24] Li L, Zhou H D, Yan J Q, Mandrus D and Keppens V 2014 *APL Mater.* **2** 110701
[25] Li L, Morris J R, Koehler M R, Dun Z L, Zhou H D, Yan J Q, D Mandrus and V Keppens 2015 *Phys. Rev. B* **92** 024109
[26] Roy S, Khan N and Mandal P 2016 *APL Mater.* **4** 026102
[27] Akamatsu H, Kumagai Y, Oba F, Fujita K, Murakami H, Tanaka K and Tanaka I 2011 *Phys. Rev. B* **83** 214421
[28] T Katsufuji and Y Tokura 1999 *Phys. Rev. B* **60** R15021
[29] Gschneidner K A Jr, Pecharsky V K, Pecharsky A O and Zimm C B 1999 *Mater. Sci. Forum* **315–317** 42
[30] Jia Y S, Wang Q, Qi Y and Ling L W 2017 *J. Alloys Compd.* **726** 1132
[31] Oleaga A, Salazar A, Prabhakaran D, Cheng J G and J S Zhou 2012 *Phys. Rev. B* **85** 184425
[32] Wu Y D, Qin Y L, Ma X H, Li R W, Wei Y Y and Zi Z F 2019 *J. Alloys Compd.* **777** 673
[33] Banerjee S K 1964 *Phys. Lett.* **12** 16
[34] Chandra S, Biswas A, Datta S, Ghosh B, Siruguri V, Raychaudhuri A K, M H Phan and Srikanth H 2012 *J. Phys.: Condens. Matter* **24** 366004